



# A new technique to estimate regional irrigation water demand and driving factor effects using an improved SWAT model with LMDI factor decomposition in an arid basin

Minzhong Zou, Shaozhong Kang\*, Jun Niu, Hongna Lu

Center for Agricultural Water Research in China, China Agricultural University, Beijing, 100083, China

## ARTICLE INFO

### Article history:

Received 7 September 2017

Received in revised form

28 February 2018

Accepted 5 March 2018

Available online 10 March 2018

### Keywords:

Irrigation water demand

SWAT model

LMDI factor decomposition

Driving factor effects

Arid region

## ABSTRACT

To figure out the driving factors of irrigation water demand and an effective way for relieving the sharp contradiction between the supply and demand of agriculture water resources in the Heihe River basin of Northwest China, a conventional method in estimating irrigation water demand was modified by incorporating the simulations of Soil and Water Assessment Tool (SWAT) model with its distributed hydrological response units (HRUs). Simultaneously, a new factor decomposition model for irrigation water demand was created using the extended Kaya identity. Moreover, the additive and multiplicative forms of the logarithmic mean Divisia index (LMDI) decomposition were used to quantify the variation of driving factors in irrigation water demand from 1985 to 2014. The results show that total irrigation water demand in this arid region had increased by  $3.249 \times 10^8 \text{ m}^3$  over the past 30 years. These contributions are arising from the following four driving factors - planting scale, planting pattern, climate change and water saving technology (e.g., drip irrigation, sprinkler irrigation, etc.) with respective contribution of irrigation water demand of  $1.981 \times 10^8 \text{ m}^3$ ,  $0.933 \times 10^8 \text{ m}^3$ ,  $1.523 \times 10^8 \text{ m}^3$  and  $-1.188 \times 10^8 \text{ m}^3$ . The corresponding average contribution rates of these driving factors are 60.96%, 28.72%, 46.86% and -36.53%, respectively. Although the effects of the four drivers on the irrigation water demand for various crops over three periods (i.e., 1985–1994; 1995–2004; 2005–2014) are inconsistent, both the planting scale and the cropping pattern increase the irrigation water demand. Water saving technologies as known have inhibited water demand, but climate change turns out to increase the demand and then inhibit it. Therefore, to reduce the irrigation water demand and develop a proper irrigation water planning in Heihe River basin, it is beneficial to regulate the scale of agricultural development, adjust the agriculture pattern by reducing the area planted with crops that consume relatively large amounts of water (i.e. spring corn and vegetables), identify agricultural water saving potential and decrease the impact of climate change.

© 2018 Elsevier Ltd. All rights reserved.

## 1. Introduction

China is one of the most water-scarce countries in the world. Limited water resources heavily constrain China's economic and social development (Cheng et al., 2009; Guo and Shen, 2016; Kang et al., 2017; Shen et al., 2013), especially in the country's arid and semi-arid regions (Du et al., 2015; Ma et al., 2012; Vorosmarty et al., 2000). Within agriculture (China's biggest water consumer), the irrigation accounts for about 90% of agricultural water use (Kang et al., 2017). The agricultural water shortage may be intensified

due to continuing economic development, rapid population increase and the impact of global climate change (Du et al., 2015; Kang et al., 2017).

The demand for irrigation water is mainly influenced by climate change, the scale and patterns of crop planting, and the use of water saving technologies. Climate change affects the demand for irrigation by altering crop water demand. Appropriate planting scale and planting patterns can effectively reduce irrigation water demand. Water saving technology such as drip irrigation can provide efficient irrigation equipment and thus improve the efficiency of irrigation methods to reduce irrigation water demand (Xie and Su, 2017). Tillage and cultivation practices, such as the use of plastic film mulch, can prevent irrigation water from losing (Kang et al.,

\* Corresponding author.

E-mail address: [kangsz@cau.edu.cn](mailto:kangsz@cau.edu.cn) (S. Kang).

2017). Due to the deficit of irrigation water and the limited existing water resources, an effective way to reduce irrigation water demand is urgent. Therefore, exploring the factors that influence the irrigation water demand, and quantifying their contribution to that demand could provide insights on controlling the scale of agriculture. Moreover, this can improve agricultural water conservation practices and promote more sustainable agriculture to secure food production in China.

Demand for irrigation water is determined by factors such as net irrigation water demand, planting practices, regional crop selections and the efficiency of irrigation water use (Shen et al., 2013; Wu and Chen, 2013). Net irrigation water demand is closely related to the water demand of a crop and the need for an effective supply of water during the crop growth period. Conventional methods to estimate effective water supply are based on the relationship between monthly mean precipitation and monthly crop water demand, neglecting the effects of the infiltration rate and the precipitation intensity (Wu and Chen, 2013). When the infiltration rate is low, and precipitation intensity is high, a considerable amount of water may be lost through surface streamflow (runoff), which was not considered by Doorenbos and Pruitt (1977). Seepage from the root zone and subsurface lateral flow can also result in water loss, which was not reported by Doorenbos and Pruitt (1977). These components of the hydrological process can be monitored by a distributed hydrological model to accurately calculate effective precipitation.

The Soil and Water Assessment Tool (SWAT) is a distributed hydrological model that has been widely used in hydrologic cycle models (Arnold et al., 1998). There have been many studies on irrigation water demand for single crops (Chung et al., 2011; Liu et al., 2013), but aggregate total regional irrigation water demand has not been comprehensively modeled. We incorporate the attributes of the distributed hydrological response calculation units in SWAT, taking advantage of its distributed crop water demand calculation and the accuracy of effective precipitation calculation, to estimate the change in irrigation water demand for each crop (i.e., spatially) and the total irrigation water demand for the crop growth period (i.e., temporally). Many published studies also reported the relationship between irrigation water demand and the influencing factors. Hu et al. (2014) found that effective precipitation was a significant predictor of irrigation water demand for winter wheat in Northern China by analyzing correlations between meteorological factors and irrigation water demand. By using multivariate linear regression analysis, Ma et al. (2011) concluded that the main driving factors of irrigation water demand were the wheat and vegetable acreages in the North China Plain. Ma et al. (2012) created an agricultural net irrigation water model by analyzing the correlation between net agricultural irrigation water demand and its macroscopic driving factors (such as population, urbanization rate, irrigated area, and natural precipitation) in the Shiyang River basin. However, these studies mainly focus on the correlation between irrigation water demand and the factors that influence it, not quantifying in what magnitude they matter to irrigation. It is necessary to examine the quantity or contribution ratio of these factors to irrigation water demand.

To date, there have been developments in methods for the quantitative analysis of factors that influence the use of water resources. Of particular interest are principal component analysis, factor analysis, artificial neural network analysis, factor decomposition, and suchlike. Ang et al. (1998) used the factor decomposition method to analyze the extent of the influence of different driving factors. Note that index decomposition analysis (IDA) is a form of factor decomposition such as Laspeyres index decomposition or Divisia index decomposition that has been commonly used. There are two interrelated forms of decomposition (additive and

multiplicative) which can improve both the temporal and spatial analysis of factor variables (Xu et al., 2015; Zhang et al., 2016c). Based on Divisia index decomposition, Ang (2015) developed the logarithmic mean Divisia index (LMDI) method which has been widely used in the fields of environmental economy and energy consumption (Chong et al., 2015; Lei et al., 2012; Tursun et al., 2015). Note that LMDI decomposition effectively deals with the problem of a residual in the decomposition process and provides the logarithmic average weight equation. It also provides the advantage of using quantitative indicators and intensity indicators. Because of its flexibility, LMDI decomposition has recently been used in the management of water resources. For example, Zhao and Chen (2014) investigated the driving factors of China's agricultural water usage by LMDI decomposition and concluded that economic benefits are the most important factor that can increase water usage in China. Zhang et al. (2014) used LMDI decomposition to analyze industrial water use in the Anhui province by quantifying the water consumption of different industrial sectors and total water use. Zhang et al. (2015c) used LMDI decomposition to investigate the water resource utilization in Urumqi. They calculated the relative contribution rate of each driving factor and found that the main determiners of water demand are the level of economic development, water use efficiency, industrial water distribution methods, industrial development, and the efficiency of industrial water use. Although LMDI decomposition has been used to analyze the water resource utilization, little research is found on its application to quantify and analyze the driving factors of irrigation water demand in arid areas.

Water shortage limits socio-economic development and could cause serious ecological and environmental damage in the arid inland area of the Heihe River basin. Agricultural water consumption accounts for up to 80% of total water consumption in the region (Li et al., 2016). The processes that cause change in the demand for irrigation water in the Heihe River basin are identified in this study. Whether the current agricultural development model is effective in reducing demand for irrigation water is also evaluated, which provides a basis for promoting the health of agricultural development in the region. The main objectives of this study are: (1) to construct a regional SWAT model and modify the conventional method in estimating irrigation water demand by incorporating the simulations of SWAT with its distributed hydrological response units (HRUs) to improve the estimation of irrigation water demand on a regional scale; (2) to quantify the temporal and spatial distribution of irrigation water demand for crops in the study area from 1985 to 2014; (3) to create a decomposition model of four factors for irrigation water demand (planting scale, planting pattern, climate change and water saving technology) by using the extended Kaya identity and LMDI decomposition in order to quantify and evaluate the contribution rate of each factor; and (4) to evaluate and discuss how the key factors that drive change in irrigation water demand might be varied in order to reduce demand.

## 2. Study area

The Heihe River basin is a typical inland river basin in Northwest China, located in the middle of Hexi Corridor and the Qilian mountains, across Qinghai, Gansu and Inner Mongolia provinces (from south to north). The study area comprises the middle and upper reaches of the Heihe River basin, from the source of the Heihe River (in the Qilian mountains) to Zhengyixia (Fig. 1). The upper reach of the Heihe River is in the south of the Qilian mountains, at altitudes of 1680 m–5280 m and covers an area of 10 009 km<sup>2</sup>. The middle reach of the Heihe River is located between Yingluoxia and Zhengyixia, at altitudes of 1300 m–1660 m and

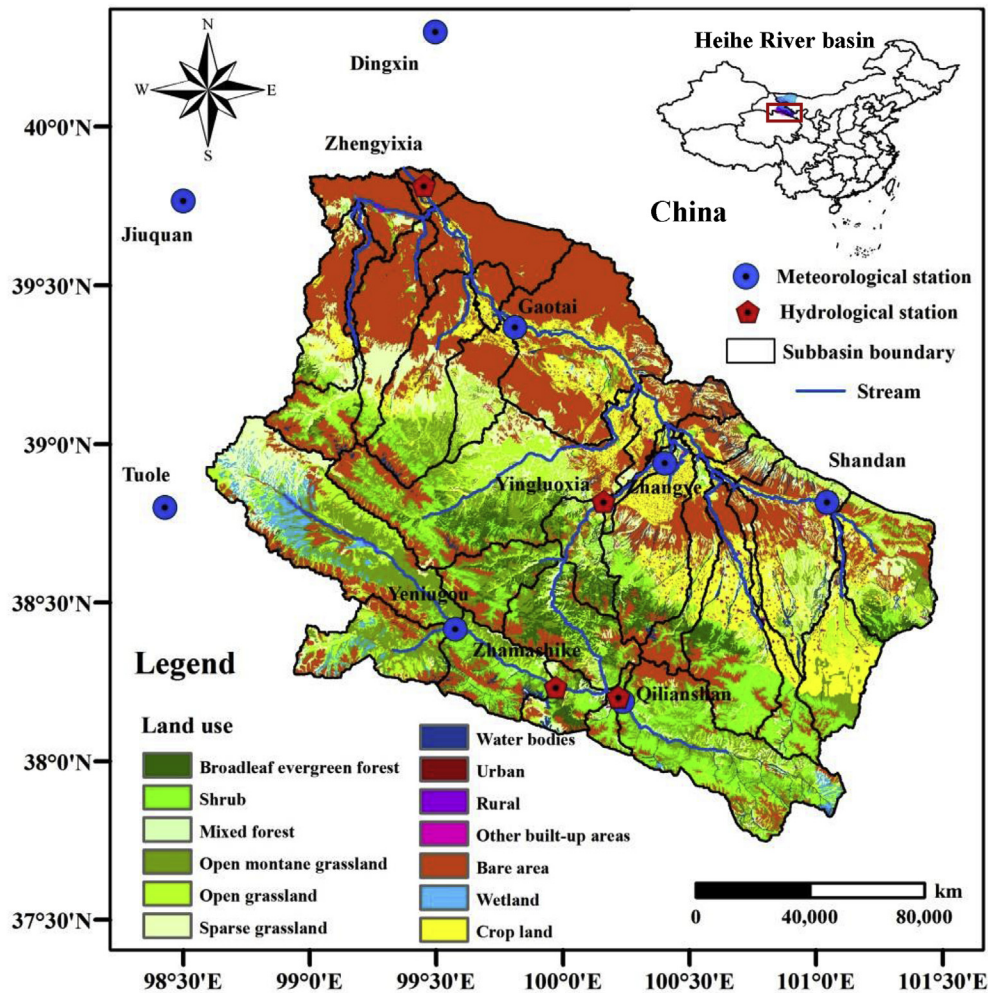


Fig. 1. Location and land cover map of the study area.

covers an area of 25 600 km<sup>2</sup>. The climate of the region is continental arid. The annual upstream precipitation in the Qilian mountains is 300–500 mm and the main vegetation types include alpine forest and grassland. The streamflow of the Heihe River drains more than 70%–80% of the total water amount in the whole basin. The annual precipitation in central Hexi Corridor is 100–250 mm. The landscape contains farmland and artificial agricultural oases which are the main water-consuming areas in the Heihe River basin. This region accounts for the majority of grain, vegetable and seed production in Northwest China, while the irrigation water relies largely on groundwater and diversion from the Heihe River (Zou et al., 2017). The cultivated land mostly concentrated in Minle County, Shandan County, Ganzhou District, Linze County and Gaotai County. Dominant crops include spring corn, spring wheat, vegetables, oil-bearing crops, cotton and alfalfa.

### 3. Data and methods

#### 3.1. Datasets

##### 3.1.1. Hydro-meteorological and geographical data

The data used for SWAT model setup and estimating irrigation water demand are listed in Table 1. The climate meteorological data at eight national meteorological stations (Fig. 1) were obtained from the China Meteorological Data Sharing Service System ([http://](http://data.cma.cn)

[data.cma.cn](http://data.cma.cn)), including daily precipitation, maximum and minimum temperature, wind speed, relative humidity, and solar radiation. The SWAT model was calibrated using the sequential uncertainty fitting algorithm (SUFI-2) procedure (Abbaspour et al., 2007) based on the monthly streamflow data from the Zhamashike and Qilianshan hydrological stations for the period 1995–2000, and the streamflow data from the Yingluoxia station for 1966–1995, all provided by the Hydrological Bureau of Gansu Province (Zhang et al., 2016a).

The geographic data used in this study include digital elevation model (DEM) that clipped from the ASTER Global DEM, soil data and land use data. The resolution of DEM is 30 m. The soil map and the land use map are both 1:1 000 000. All geographic data were obtained from the Data Management Center of the Heihe Research Program (<http://westdc.westgis.ac.cn/>).

##### 3.1.2. Agricultural management data

In this study, the growth periods and crop coefficients ( $K_c$ ) of each crop refer to those given by Duan et al. (2004). We assume that  $K_c$  takes the same value for each year. The values are shown in Table 2. The irrigation water use efficiency applied to entire study area is the average value of typical irrigation region, obtained from the Zhangye Water Conservancy Yearbook. The planted area of each crop and tillage data were gained from the China Economic and Social Development Statistics Database (<http://tongji.cnki.net/kns55/>

**Table 1**

Description of data used to configure the SWAT model and calculate irrigation water demand.

Data	Application	Data description and configuration details	Source
Digital elevation model (DEM) and digitised stream network	Sub-basin delineation	30m resolution. Used to define three slope classes: 0–9, 9–25 and > 25%	Data Management Center of the Heihe Research Program ( <a href="http://westdc.westgis.ac.cn/">http://westdc.westgis.ac.cn/</a> )
Land use	HRU definition	1:1000 thousand scale. 13 basic land-cover categories	Data Management Center of the Heihe Research Program ( <a href="http://westdc.westgis.ac.cn/">http://westdc.westgis.ac.cn/</a> )
Soil data	HRU definition	1:1000 thousand scale. 43 soil types. Properties were quantified based on measurements or estimated using the SPAW and EXCEL software	Data Management Center of the Heihe Research Program ( <a href="http://westdc.westgis.ac.cn/">http://westdc.westgis.ac.cn/</a> )
Meteorological data	Meteorological forcing	Daily maximum and minimum temperature, daily mean relative humidity, daily global solar radiation, daily surface wind speed and precipitation	China Meteorological Data Sharing Service System ( <a href="http://data.cma.cn">http://data.cma.cn</a> )
Monthly streamflow data	Calibration and validation	Zhamashike and Qilianshan hydrological stations (1995–2000)	Hydrological Bureau of Gansu Province
Agricultural management data	Irrigation water demand calculation	Yingluoxia hydrological station (1966–1995) The growth periods and crop coefficients ( $K_c$ ) of different crops, irrigation water use coefficient, planted area of each crop and tillage data	Duan et al. (2004) Zhangye Water Conservancy Yearbook China Economic and Social Development Statistics Database ( <a href="http://tongji.cnki.net/kns55/index.aspx">http://tongji.cnki.net/kns55/index.aspx</a> ) Gansu Development Yearbook Gansu Rural Yearbook

[index.aspx](#)), the *Gansu Development Yearbook* and the *Gansu Rural Yearbook*.

### 3.2. Methods

#### 3.2.1. SWAT model and its improvement

The SWAT is a robust distributed hydrological model. It has been widely used in hydrologic cycle simulation and research in China and has been successfully used to model the middle and upper reaches of the Heihe River basin (Li et al., 2010; Lu et al., 2015; Zhang et al., 2015b; Zhang et al., 2016a,b; Zou et al., 2017). Fig. 2 shows the primary procedures of data processing, model setup, parameter estimation and model application using the SWAT. Stream network information was derived from DEM and the watershed was divided into smaller sub-basins. The size of sub-basins can be calculated by setting the area of the smallest catchment area. In the end, the catchment area was set to 64 561 ha, and the area in the upper and middle reaches of Heihe River basin was divided into 35 sub-basins (Fig. 1). Then, by combining 43 soil types and 13 land use types (Table 1), the sub-basins were further sub-divided into 828 HRUs. The responses of each HRU in terms of water transformation and loss are determined individually, aggregated at the sub-basin scale, and routed to the associated reach catchment outlets throughout the channel network. SWAT represents the local water balance through four storage volumes: snow, soil profile, shallow and deep aquifers. The soil water balance equation is fundamental for hydrological modeling. The simulated processes include surface streamflow, infiltration, evaporation, plant water uptake, lateral flow, and percolation to shallow and deep aquifers. ArcSWAT 2009 was implemented to simulate the surface

streamflow. For the streamflow calculation, the Soil Conservation Service curve number (SCS–CN) was used in each HRU. The river channel accumulation method based on the continuity equation is used to calculate the water flow through the main channel. The technical details of the model were reported by Neitsch et al. (2002, 2005) and Gassman et al. (2007).

Importantly, the large elevation differences in the Heihe River basin result in significant variations in precipitation and temperature. Therefore, when calculating the lapse rates of precipitation and temperature for each sub-basin, the watershed was divided into altitude zones at a 200 m interval to take account of the variability of precipitation and temperature induced by topographic changes. After the precipitation and temperature of each altitude zone were obtained, the average precipitation and temperature of each sub-basin were modified by finding a weighted average based on the relative area of each altitude zone in the sub-basin. The following equations are used for the precipitation and temperature calculations of the altitude zones (Hao et al., 2013).

$$P_b = P + (E_b - E_{gage}) \cdot P_{laps} \quad (1)$$

$$T_{b,max} = T_{max} + (E_b - E_{gage}) \cdot T_{laps} \quad (2)$$

$$T_{b,min} = T_{min} + (E_b - E_{gage}) \cdot T_{laps} \quad (3)$$

where  $P_b$  is the precipitation in altitude zone  $b$ , mm;  $P$  is the precipitation recorded at the weather station, mm;  $E_b$  is the elevation of the mid-point elevation of the altitude zone  $b$ , km;  $E_{gage}$  is the elevation of the weather station, km;  $T_{b,max}$  and  $T_{b,min}$  are

**Table 2**

Crop coefficients of the major crops in the Heihe River basin.

Crops	Development stage				Sowing (mm/dd)	Harvesting (mm/dd)	Total (days)
	Initial	Developing	Middle	Late			
Spring corn	0.23	0.23–1.20	1.20	1.20–0.35	4/13	9/26	167
Spring wheat	0.23	0.23–1.16	1.16	1.16–0.40	3/13	7/17	127
Cotton	0.27	0.27–1.20	1.20	1.20–0.70	4/11	10/11	184
Oil-bearing crops	0.31	0.31–1.15	1.15	1.15–0.35	6/14	9/29	108
Vegetables (twice planting)	0.36	0.36–1.35	1.35	1.35–0.38	3/15	8/14	150
Other crops (i.e. barley, potato, etc.)	0.27	0.28–1.15	1.15	1.15–0.75	4/14	8/18	127

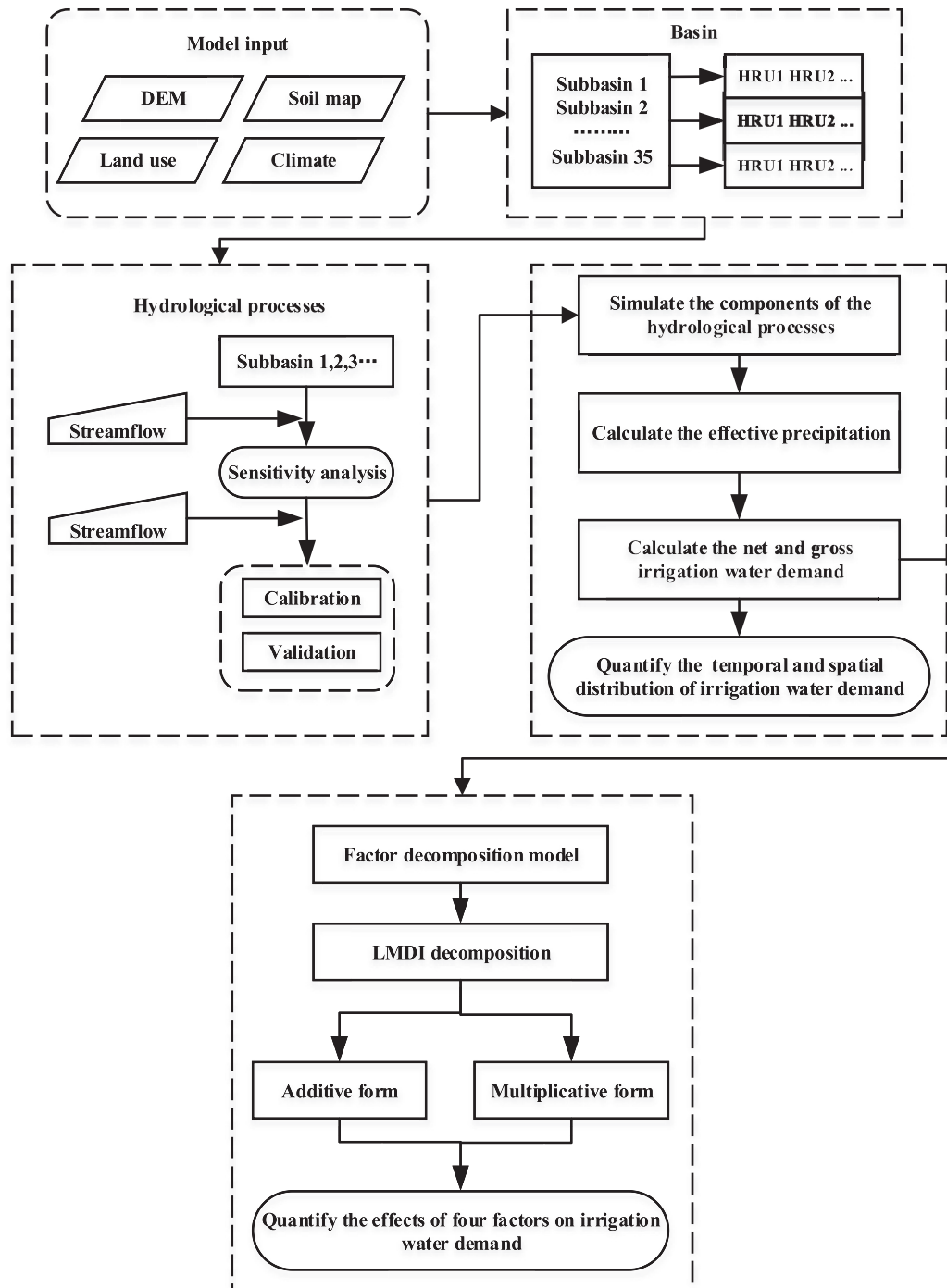


Fig. 2. Flow chart of creating the SWAT model and estimating the irrigation water demand and driving factor effects.

respectively the maximum and minimum temperatures of altitude zone  $b$ ,  $^{\circ}\text{C}$ ;  $T_{\max}$  and  $T_{\min}$  are respectively the maximum and minimum temperatures of the weather station,  $^{\circ}\text{C}$ ;  $P_{\text{laps}}$  is the lapse rate of precipitation,  $\text{mm}/\text{km}$ ;  $T_{\text{laps}}$  is the lapse rate of temperature,  $^{\circ}\text{C}/\text{km}$ . And the  $T_{\text{laps}} = -5.2^{\circ}\text{C}/\text{km}$  was determined by establishing a linear relationship between the multi-year average temperature and the altitude of the weather stations.  $P_{\text{laps}}$  refers to the value given by Zhang et al. (2016a) as  $115 \text{ mm}/\text{km}$ .

### 3.2.2. Sensitivity analysis, model calibration and validation

The Latin hypercube one-factor-at-a-time (LH-OAT) method was used for sensitivity analysis (van Griensven et al., 2006). According to previous literature on sensitivity analysis of SWAT model parameters (van Griensven et al., 2006; Kannan et al., 2008; Zhang et al., 2010) and the situation of the middle and upper reaches of the Heihe River basin, 15 parameters were selected for sensitivity analysis. The SUFI-2, which forms part of SWAT-CUP (Abbaspour et al., 2007), was used for the 10 most sensitive parameters

optimization. For calibration, the relationship between annual evaporation and streamflow had been adjusted until the values of total evaporation, precipitation and streamflow of the simulated watershed were reasonable. The streamflow data was measured following the sequence of Qilianshan, Zhamashike, and Yingluoxia station. This was because the Yingluoxia is downstream of the other two, and any inaccurate upstream parameters would affect the accuracy of the downstream parameters. A two-year period was used to warm up the SWAT model for both sensitivity analysis and calibration. The calibration period for the Qilianshan and Zhamashike stations was 1995–1998 and the validation period was 1999–2000. The calibration period for the Yingluoxia station was 1966–1984, whereas the years from 1985 to 1995 were used for validation.

### 3.2.3. Calculation of irrigation water demand

In this study, the details of calculating the potential crop water demand, crop water demand, net irrigation water demand, effective precipitation and gross irrigation water demand for each crop are given in [Appendix A](#).

### 3.2.4. Analysis of driving factor effects on irrigation water demand

#### (1) The factor decomposition model of irrigation water demand

By using the extended Kaya identity, developed by [Xie and Su \(2017\)](#), the decomposition model of irrigation water demand is:

$$W = \sum_j \sum_i W_{ij} = \sum_j \sum_i \frac{W_{ij}}{\eta_j} = \sum_j \sum_i A_j \cdot \frac{A_{ij}}{A_j} \cdot \frac{w_{ij}}{A_{ij}} \cdot \frac{1}{\eta_j} = \sum_j \sum_i A_j \cdot \alpha_{ij} \cdot I_{ij} \cdot C_j \quad (4)$$

where  $W_{ij}$  and  $w_{ij}$  are respectively gross irrigation water demand and net irrigation water demand for crop  $i$  in year  $j$ ,  $10^8 \text{ m}^3$ ;  $A_{ij}$  is the planted area in year  $j$ ,  $10^4 \text{ ha}$ , reflecting the planting scale of the year  $j$ ;  $\alpha_{ij} = \frac{A_{ij}}{A_j}$  is the ratio of the planted area of crop  $i$  to the total area in year  $j$ , reflecting the cropping pattern in year  $j$ ;  $I_{ij} = \frac{w_{ij}}{A_{ij}}$  is the net irrigation water demand per unit area of crop  $i$  in year  $j$ ,  $\text{mm}$  (the value of  $I_{ij}$  is related to potential crop water demand, the crop coefficient, and effective precipitation for the growth period. As the potential crop water demand is calculated by the Penman-Monteith equation,  $I_{ij}$  is affected by climate change. Thus  $I_{ij}$  can reflect the impact of climate change on irrigation water demand);  $C_j = \frac{1}{\eta_j}$ , where  $\eta_j$  is the irrigation water use efficiency for year  $j$  (its value is influenced by factors such as irrigation project construction, field water-saving projects, irrigation technology, and soil water storage characteristics. Thus, it reflects the impact of water saving practices on irrigation water demand).

#### (2) LMDI decomposition of irrigation water demand

There are two forms of LMDI decomposition, additive and multiplicative ([Ang, 2015](#)). Each form can be transformed into the other by a particular method. After a detailed derivation given in [Appendix A](#), the additive form of LMDI decomposition for irrigation water demand can be expressed as:

$$\Delta W_{tot} = W^t - W^0 = \Delta W_A + \Delta W_\alpha + \Delta W_I + \Delta W_C \quad (5)$$

where  $\Delta W_{tot}$  is the change in irrigation water demand, and is the sum of the factors which influence demand (the driving factors),

that is, the total effect of the additive decomposition,  $10^8 \text{ m}^3$ ;  $W^0$  is the irrigation water demand for the base year,  $10^8 \text{ m}^3$ ;  $W^t$  is the irrigation water demand for year  $j$ ,  $10^8 \text{ m}^3$ ;  $\Delta W_A$  is the effect of changes in planting scale,  $10^8 \text{ m}^3$ ;  $\Delta W_\alpha$  is the effect of changes in planting patterns,  $10^8 \text{ m}^3$ ;  $\Delta W_I$  is the effect of climate change,  $10^8 \text{ m}^3$ ;  $\Delta W_C$  is the effect of changes in water saving technology,  $10^8 \text{ m}^3$ . The driving factors in the additive decomposition of irrigation water demand are calculated as follows:

$$\Delta W_A = \sum_j \sum_i \frac{W_{ij}^t - W_{ij}^0}{\ln W_{ij}^t - \ln W_{ij}^0} \ln \left( \frac{A_j^t}{A_j^0} \right) \quad (6)$$

$$\Delta W_\alpha = \sum_j \sum_i \frac{W_{ij}^t - W_{ij}^0}{\ln W_{ij}^t - \ln W_{ij}^0} \ln \left( \frac{\alpha_{ij}^t}{\alpha_{ij}^0} \right) \quad (7)$$

$$\Delta W_I = \sum_j \sum_i \frac{W_{ij}^t - W_{ij}^0}{\ln W_{ij}^t - \ln W_{ij}^0} \ln \left( \frac{I_{ij}^t}{I_{ij}^0} \right) \quad (8)$$

$$\Delta W_C = \sum_j \sum_i \frac{W_{ij}^t - W_{ij}^0}{\ln W_{ij}^t - \ln W_{ij}^0} \ln \left( \frac{C_j^t}{C_j^0} \right) \quad (9)$$

In the additive decomposition, a factor having value  $> 0$  shows that it drives an increase in irrigation water demand, and a factor having value  $< 0$  drives a decrease in irrigation water demand. The greater the absolute value of a factor, the greater is the influence of that factor on irrigation water demand. A factor with zero value has no significant effect on irrigation water demand.

Simultaneously, the multiplicative LMDI decomposition for irrigation water demand can be estimated as follows:

$$D_{tot} = \frac{W^t}{W^0} = D_A \cdot D_\alpha \cdot D_I \cdot D_C \quad (10)$$

where  $D_{tot}$  is the ratio of irrigation water demand for year  $j$  to the base year, which is equal to the product of the four driving factors, that is, the total effect of the multiplicative decomposition;  $D_A$  is the planting scale factor;  $D_\alpha$  is the planting pattern factor;  $D_I$  is the climate change factor;  $D_C$  is the water saving technology factor. The multiplicative effect of irrigation water demand can be calculated:

$$D_A = \exp \left\{ \sum_j \sum_i \left[ \frac{(W_{ij}^t - W_{ij}^0) / (\ln W_{ij}^t - \ln W_{ij}^0)}{(W^t - W^0) / (\ln W^t - \ln W^0)} \ln \left( \frac{A_j^t}{A_j^0} \right) \right] \right\} \quad (11)$$

$$D_\alpha = \exp \left\{ \sum_j \sum_i \left[ \frac{(W_{ij}^t - W_{ij}^0) / (\ln W_{ij}^t - \ln W_{ij}^0)}{(W^t - W^0) / (\ln W^t - \ln W^0)} \ln \left( \frac{\alpha_{ij}^t}{\alpha_{ij}^0} \right) \right] \right\} \quad (12)$$

$$D_I = \exp \left\{ \sum_j \sum_i \left[ \frac{(W_{ij}^t - W_{ij}^0) / (\ln W_{ij}^t - \ln W_{ij}^0)}{(W^t - W^0) / (\ln W^t - \ln W^0)} \ln \left( \frac{I_{ij}^t}{I_{ij}^0} \right) \right] \right\} \quad (13)$$

$$D_C = \exp \left\{ \sum_j \sum_i \left[ \frac{(W_{ij}^t - W_{ij}^0) / (\ln W_{ij}^t - \ln W_{ij}^0)}{(W^t - W^0) / (\ln W^t - \ln W^0)} \ln \left( \frac{C_j^t}{C_j^0} \right) \right] \right\} \quad (14)$$

In the multiplicative decomposition form, a factor having value  $> 1$  shows that it drives an increase in irrigation water demand, and a factor having value  $< 1$  shows that it drives a decrease in irrigation water demand. The more the value of a factor deviates from 1, the greater the influence of that factor on irrigation water demand. A factor with a value equal to 1 has no significant influence on irrigation water demand.

### 3.2.5. Statistical analysis

In this study, the Kendall's rank correlation test was projected to reveal the trends of irrigation water demand and the driving factors. A detailed introduction to this approach is given by Kendall and Stuart (1964) and Mann (1945). Moreover, the nonparametric change point test method reported by Pettitt (1979) was also applied to testify whether the mean of a variable would change crossing a certain point of time.

## 4. Results and discussion

### 4.1. Evaluation of SWAT model performance

In this study, the simulated streamflow curves of the three hydrological stations were monthly compared with the observed

values. In general, the quantity and trend of the observed values were consistent with those of the simulated values, and the SWAT model well simulated the seasonal dynamics of streamflow (Fig. 3). For the calibration period, values of  $NSE$  at the Zhamashike and Qilianshan stations were 0.90 and 0.87 and  $R^2$  was 0.92 and 0.88, respectively. For the validation period  $NSE$  values at the two stations were 0.88 and 0.85, and  $R^2$  were 0.90 and 0.89, respectively. For the Yingluoxia station, the range of the  $NSE$  was 0.77–0.79, and the range of  $R^2$  was 0.83–0.85,  $RB$  and  $RMSE$  were relatively small during the calibration and validation periods (Table 3). In order to represent the variability of temperature and precipitation induced by topographic changes, the lapse rate of temperature of  $-5.2^\circ\text{C}/\text{km}$  and the average value given by Zhang et al. (2016a) of  $115\text{ mm}/\text{km}$  were analyzed based on the observed temperature and precipitation dataset. This process greatly improves the model performance by offsetting the negative effect resulting from the large study area and limited data. The simulation results for Zhamashike station and Qilianshan station were better than that for Yingluoxia station, which may due to their remote locations and the relatively small effect of human activity around. However, the reservoir that changed the regime of streamflow affected the Yingluoxia station data (Zhang et al., 2016b). The SWAT model does not consider the

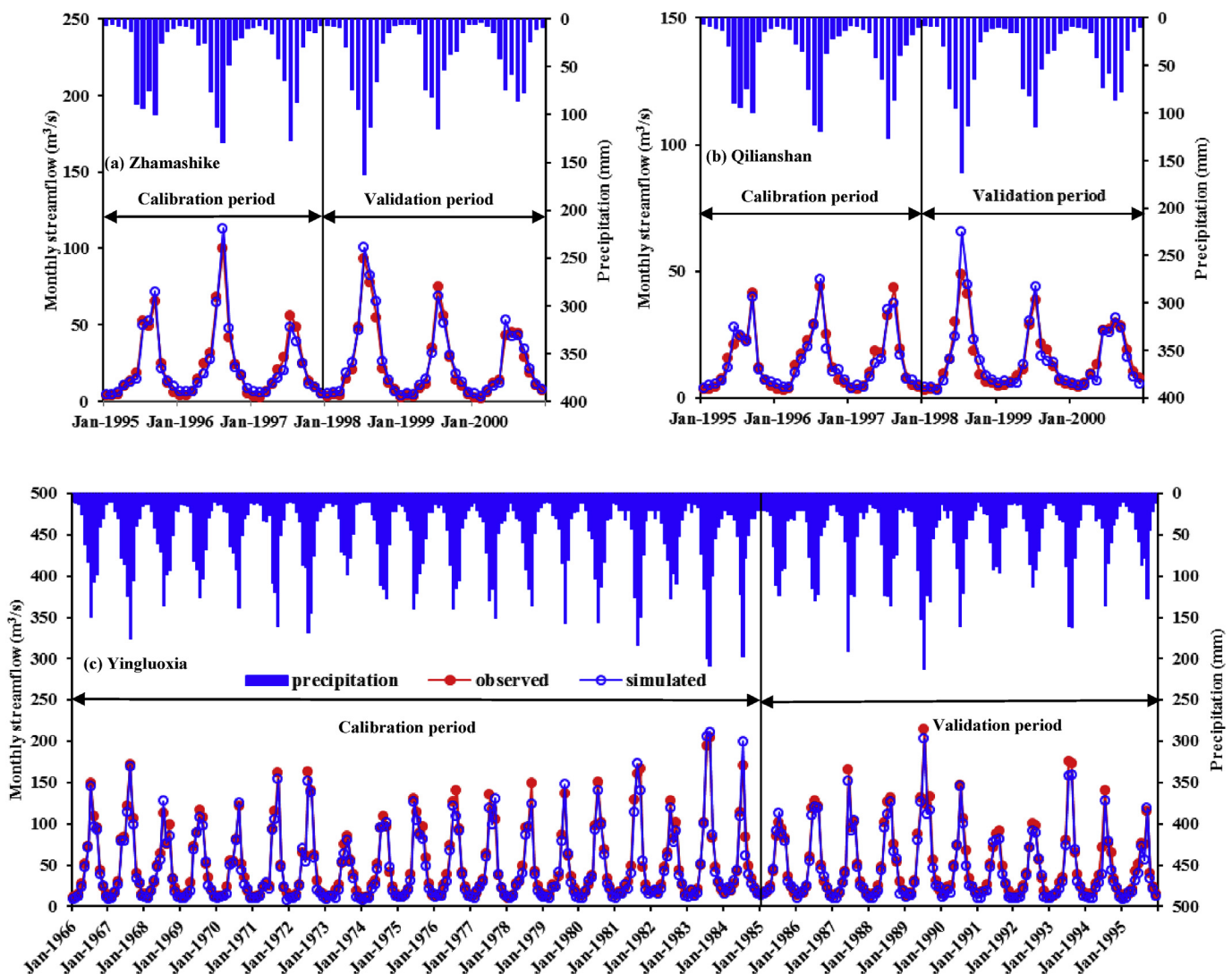


Fig. 3. Simulated and observed streamflows for calibration and validation periods: (a) Zhamashike station; (b) Qilianshan station; (c) Yingluoxia station.

**Table 3**

Streamflow simulation results at three hydrological stations for the calibration and validation periods.

Station	Calibration period				Validation period			
	NSE	R <sup>2</sup>	RB	RMSE (m <sup>3</sup> /s)	NSE	R <sup>2</sup>	RB	RMSE (m <sup>3</sup> /s)
Zhamashike	0.90	0.92	−0.45	4.41	0.88	0.90	0.17	4.04
Qilianshan	0.87	0.88	−0.36	3.67	0.85	0.89	0.23	3.98
Yingluoxia	0.79	0.85	−0.92	7.02	0.77	0.83	−1.19	7.34

influence of the reservoir because of little relevant information and potential of low accuracy of the simulation. Nevertheless, according to the criteria proposed by Moriasi et al. (2007), the simulation results for the three hydrological stations all fall within the range of *good* to *very good*, conclusion based on which also agrees with other studies in the same basin (Lu et al., 2015; Zhang et al., 2015b, Zhang et al., 2016a).

#### 4.2. The temporal and spatial distribution of irrigation water demand

The total irrigation water demand in study area increased from  $17.463 \times 10^8 \text{ m}^3$  in 1985 to  $30.599 \times 10^8 \text{ m}^3$  in 2014. The average growth amount over the 30 years was  $0.453 \times 10^8 \text{ m}^3/\text{year}$ , showing a considerable increasing trend (Fig. 4, Table 4). A sudden change in demand occurred in 2000 (Table 5), which is closely related to an alteration of crop pattern. In detail, the increased area of crops, such as spring corn and vegetables, resulted in larger water demand in the region (Fig. 6a and b, Table 4). The average annual growth rate of spring corn, cotton, vegetables and other crops in the upper and middle reaches of Heihe River basin increased by  $0.328 \times 10^8 \text{ m}^3/\text{year}$ ,  $0.006 \times 10^8 \text{ m}^3/\text{year}$ ,  $0.117 \times 10^8 \text{ m}^3/\text{year}$  and  $0.067 \times 10^8 \text{ m}^3/\text{year}$ , respectively. There were abrupt increases in water demand in 2000, 1996, 1999 and 2000 (Table 5), which due to that larger areas were planted with spring corn, cotton, vegetables and other crops, and that climate change induced the increase in net irrigation water demand per unit area of crop (Fig. 6c, Table 4). A significant decreasing trend was found in the irrigation water demand of spring wheat and oil-bearing crops. The average rates for the 30-year period decreased

from  $0.044 \times 10^8 \text{ m}^3/\text{year}$  to  $0.021 \times 10^8 \text{ m}^3/\text{year}$ . The rates were reduced in 1997 and 2001 (Table 5), which mainly caused by the largely reduced area of spring wheat and oil-bearing crops (Fig. 6a, Table 4).

Fig. 5 shows the spatial distribution of average total irrigation water demand over the past 30 years in the middle and upper reaches of the Heihe River basin. It reveals that the total irrigation water demand was unevenly distributed, increasing from southwest to northeast. The maximum value was  $2.8981 \times 10^8 \text{ m}^3$  in middle area, and the minimum value was  $0.0008 \times 10^8 \text{ m}^3$  in upper area. This is mainly due to the significant differences on indexes of precipitation, temperature, soil quality, planting pattern and other conditions in study area. Cultivated land was mostly established in the middle reaches where the mainstream of the Heihe River flows past. Note that the upper area is dominant by alpine forest and grassland with little areas of plantable land (Fig. 1). In these middle reaches, the crops such as corn and vegetables that consume relatively large amounts of water are mainly planted (Li et al., 2016). Further, the annual precipitation in the upper reaches is 200–250 mm more, and the annual average temperature is 6–8 °C lower than that in the middle reaches (Zhang et al., 2015a), which result in substantially lower potential crop water demand in this area.

Empirical formulas are generally adopted to estimate the effective precipitation, but inconsistent results are obtained from these formulas (Mohan et al., 1996). This may be due to that the effective precipitation is difficult to precisely calculate without considering the influence of complicated factors such as precipitation characteristics, soil texture, and crop type. As an analytical model, the SWAT model was used to simulate the hydrological process components such as surface streamflow, lateral flow, and seepage in this study. When considering the effects of precipitation intensity and infiltration rate, the errors caused by effective precipitation calculation were reduced significantly by combining with the properties of SWAT distributed hydrological response unit. The accuracy of regional irrigation water demand calculation was largely improved. In addition, the results show that the Heihe River basin is now facing a severe shortfall in demand for agricultural water use. Given above, the effects of various driving factors on irrigation water demand by creating a new decomposition model (joint the extended Kaya identity and LMDI decomposition) were

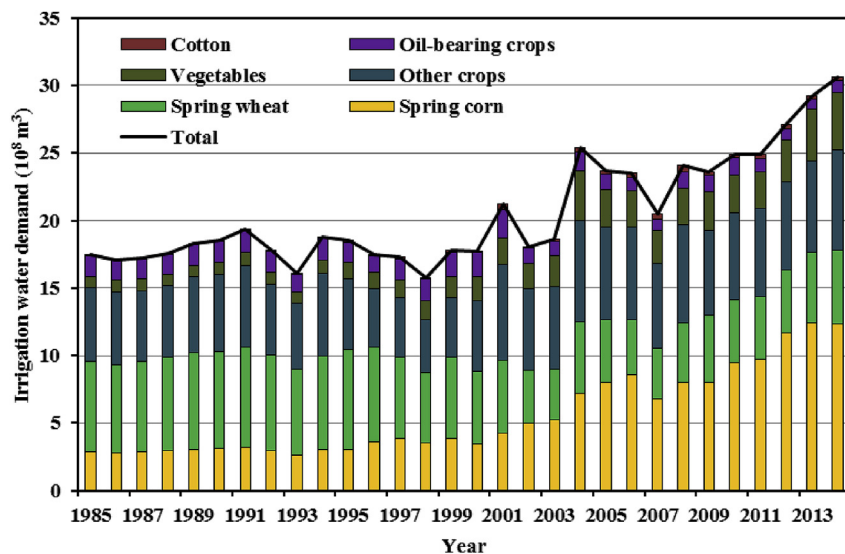


Fig. 4. Annual variation of irrigation water demand for different crops.

**Table 4**  
Kendall test of irrigation water demand and its driving factors for different crops; N-values are values of the test statistic from the Kendall trend test of the regional averaged data; ↑ and ↓ indicate an increasing or decreasing trend, respectively; \* and \*\* indicate the significance at the 0.05 and 0.01 levels, respectively.

Indicator	Spring corn		Spring wheat		Cotton		Oil-bearing crops		Vegetables		Other crops		Total	
	N-value	Trend	N-value	Trend	N-value	Trend	N-value	Trend	N-value	Trend	N-value	Trend	N-value	Trend
Irrigation water demand	6.619	↑**	−3.943	↓**	5.227	↑**	−3.372	↓**	6.762	↑**	3.336	↑**	4.906	↑**
Planting scale	6.940	↑**	−3.265	↓**	5.406	↑**	−3.015	↓**	7.083	↑**	3.586	↑**	6.762	↑**
Planting pattern	6.512	↑**	−5.370	↓**	4.978	↑**	−4.228	↓**	6.298	↑**	−1.338	↓	—	—
Crop water demand	3.122	↑**	2.494	↑*	2.658	↑**	4.585	↑**	3.729	↑**	3.087	↑**	—	—
Irrigation water use efficiency	7.297	↑**	7.297	↑**	7.297	↑**	7.297	↑**	7.297	↑**	7.297	↑**	—	—

**Table 5**  
Results of change-point analysis of irrigation water demand and its driving factors for different crops.

Indicator	Spring corn	Spring wheat	Cotton	Oil-bearing crops	Vegetables	Other crops	Total
	Pettitt test	Pettitt test	Pettitt test	Pettitt test	Pettitt test	Pettitt test	Pettitt test
Irrigation water demand	2000	1997	1996	2001	1999	2000	2000
Planting scale	2001	1999	2000	2001	1999	1999	2000
Planting pattern	2001	1999	1996	2001	1999	—	—
Crop water demand	2003	2003	2003	2000	2003	2000	—
Irrigation water use efficiency	1999	1999	1999	1999	1999	1999	—

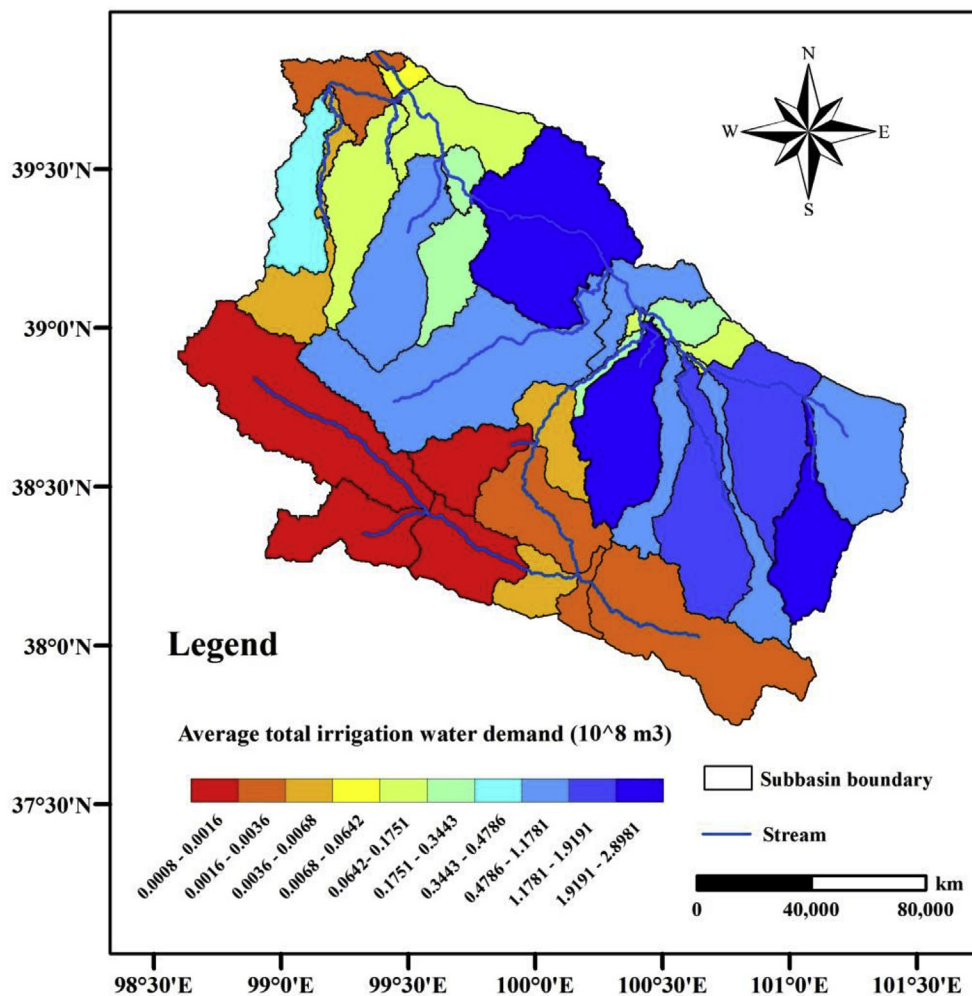


Fig. 5. The spatial distribution of average irrigation water demand during 1985–2014.

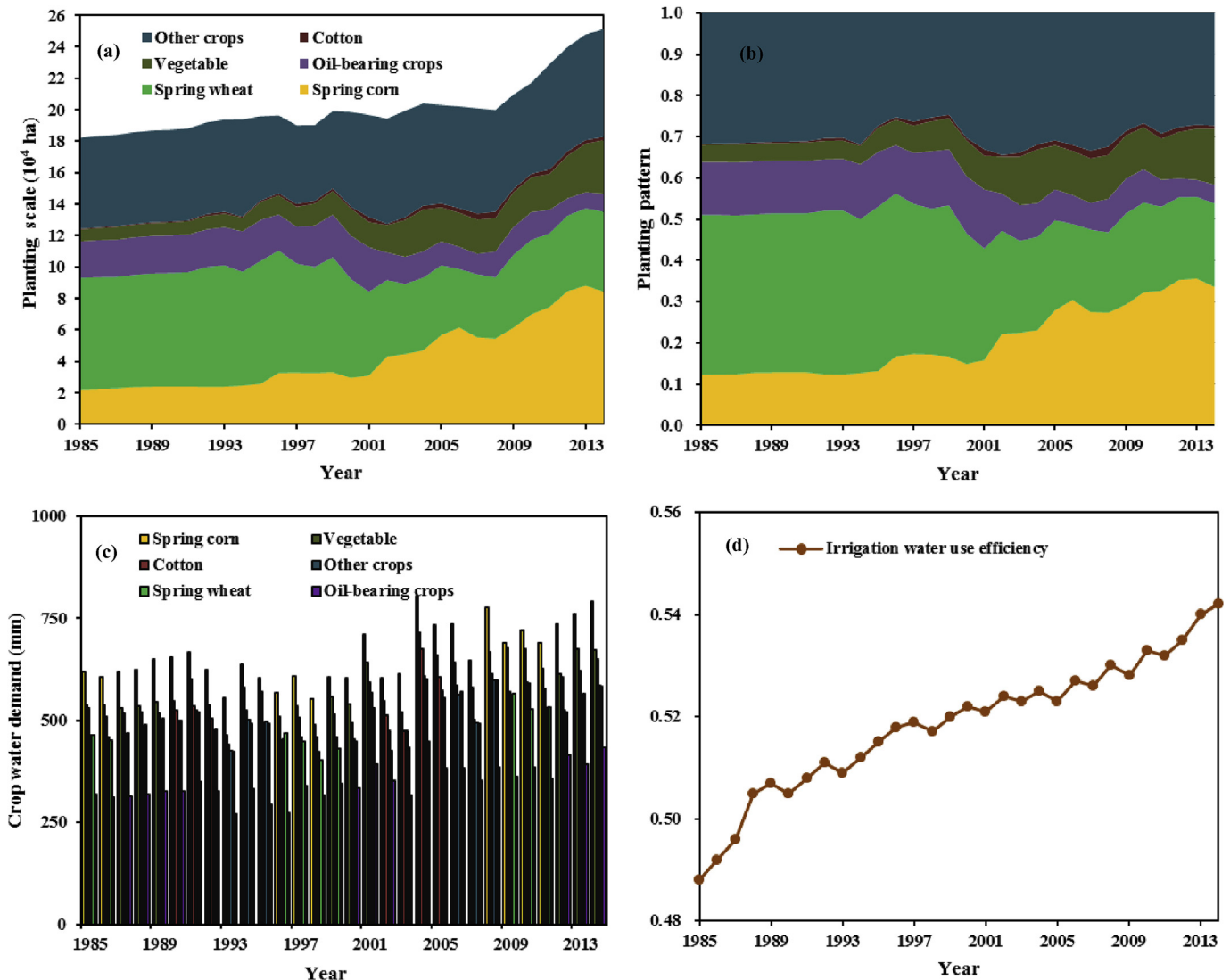


Fig. 6. Annual change in the driving factors of irrigation water demand: (a) planting areas; (b) planting patterns; (c) crop water demand; (d) irrigation water use efficiency.

quantified in order to find an effective way to reduce irrigation water demand in this study.

#### 4.3. LMDI decomposition and irrigation water demand change

The additive decomposition form of LMDI well represents the effect of the driving factors on the change in irrigation water demand, whereas the multiplicative decomposition form shows the degree of influence of those factors, that is, the relative contribution

rate (Xie and Su, 2017). The additive form from 1985 to 2014 as chosen to decompose the total change in irrigation water demand in the upper and middle reaches of Heihe River basin, and the multiplicative form was selected to decompose the change in irrigation water demand for each crop in different periods.

##### 4.3.1. Results of additive decomposition of irrigation water demand during 1985–2014

Table 6 and Fig. 7 show the additive decomposition of irrigation

**Table 6**  
Additive decomposition of irrigation water demand from 1985 to 2014 ( $10^8 \text{ m}^3$ ).

Crop	Planting scale	Planting pattern	Climate change	Water saving	Total effect
	$\Delta W_A$	$\Delta W_a$	$\Delta W_i$	$\Delta W_C$	$\Delta W_{\text{tot}}$
Spring corn	0.494	2.266	0.341	-0.274	2.827
Spring wheat	0.595	-1.695	0.413	-0.373	-1.060
Cotton	0.013	0.119	0.005	-0.007	0.129
Oil-bearing crops	0.134	-0.335	0.109	-0.087	-0.179
Vegetables	0.155	0.912	0.134	-0.087	1.114
Other crops	0.591	-0.334	0.522	-0.359	0.420
Total	1.981	0.933	1.523	-1.188	3.249

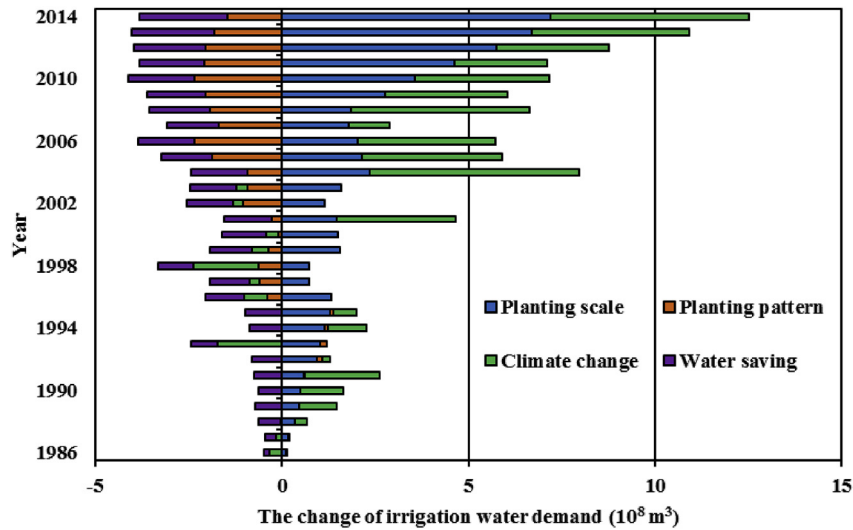


Fig. 7. Change in irrigation water demand compared with that in 1985 using LMDI additive decomposition.

water demand in the past 30 years. The results show that the total increase in irrigation water demand was  $3.249 \times 10^8 \text{ m}^3$  and that the upper and middle reaches of Heihe River basin had a certain degree of volatility. The planting scale, planting pattern, climate change, and the water saving technologies increased the respective irrigation water demand of  $1.981 \times 10^8 \text{ m}^3$ ,  $0.933 \times 10^8 \text{ m}^3$ ,  $1.523 \times 10^8 \text{ m}^3$  and  $-1.188 \times 10^8 \text{ m}^3$ . Planting scale has the greatest effect, followed by climate change, water saving technologies and planting patterns. It can be seen that planting scale, planting pattern, and climate change caused an increase in irrigation water demand, while the water saving technology induced a decrease. Due to economic constraints in the construction of irrigation canal lining, the seepage loss of irrigation water was huge in irrigation districts. Recently, the canal linings have been significantly increased due to the water conservation, reducing the loss of water seepage. Meanwhile, the canal seepage control technology, low-pressure pipeline water conveyance technology and water-saving irrigation (such as the drip irrigation, sprinkler irrigation) were developed for Heihe River basin (Wu et al., 2015), which have greatly improved the efficiency of irrigation water utilization (Fig. 6d).

Table 7 indicates that the planting scale, planting pattern and climate change were positive drivers of the growth of irrigation water demand, and their respective contribution rates were 60.96%, 28.72%, and 46.86%, while the water saving effect was a negative driver with an average contribution rate of  $-36.53\%$ . The increase in planting scale is the major driver to cause larger irrigation water demand, which is mainly due to the substantial increase in the area of cultivated land (Fig. 6a). Previous studies on the irrigation water demand related to climate change have reported that an increase in

temperature and solar radiation will lead to an increase in irrigation water demand by 10–30% (Díaz et al., 2007; Tomohisa et al., 2007). As suggested in Zhang et al. (2015a), the temperature in Heihe River basin has shown a moderately increased trend in the past 50 years, and this increase may continue in future and thus lead to a higher crop water demand (Fig. 6c). The phenomenon indicated that the change in climate is another main reason to increase irrigation water demand.

Furthermore, driving factors have different influences on the irrigation water demand. For example, the influence of the planting patterns on spring corn, cotton and vegetables were greater compared to that of the planting scale. The effects of climate change on irrigation water demand for the investigated crops were consistent, showing a positive role of climate change in promoting growth. The effects of water saving technology on reducing demand for the investigated crop were also consistent. These results suggest that, to reduce the demand for irrigation water, controlling the scale of cultivation and adjusting plant patterns are in great need. Much attention should also be paid to the impact of climate change. It is also important to construct more projects using water saving technologies that are beneficial to agricultural efficiency.

#### 4.3.2. Results of multiplicative decomposition of irrigation water demand at different stages

The results of the multiplicative decomposition are shown in Fig. 8. It can be seen in Fig. 8a that the total effect values for spring corn in the three periods (i.e., 1985–1994; 1995–2004; 2005–2014) were 1.006, 1.077 and 1.069. All values were greater than 1 and irrigation water demand showed an increasing trend. The increased change in irrigation water demand in the two periods

Table 7

Contribution rates from additive decomposition of irrigation water demand from 1985 to 2014 (%).

Crop	Planting scale $W_A$	Planting pattern $W_a$	Climate change $W_l$	Water saving $W_C$	Total effect $W_{tot}$
Spring corn	17.47	80.16	12.06	−9.68	100.00
Spring wheat	−56.10	159.88	−38.99	35.21	100.00
Cotton	9.91	92.33	3.51	−5.76	100.00
Oil-bearing crops	−74.81	187.12	−60.72	48.41	100.00
Vegetables	13.93	81.86	12.06	−7.85	100.00
Other crops	140.81	−79.48	124.23	−85.57	100.00
Total	60.96	28.72	46.86	−36.53	100.00

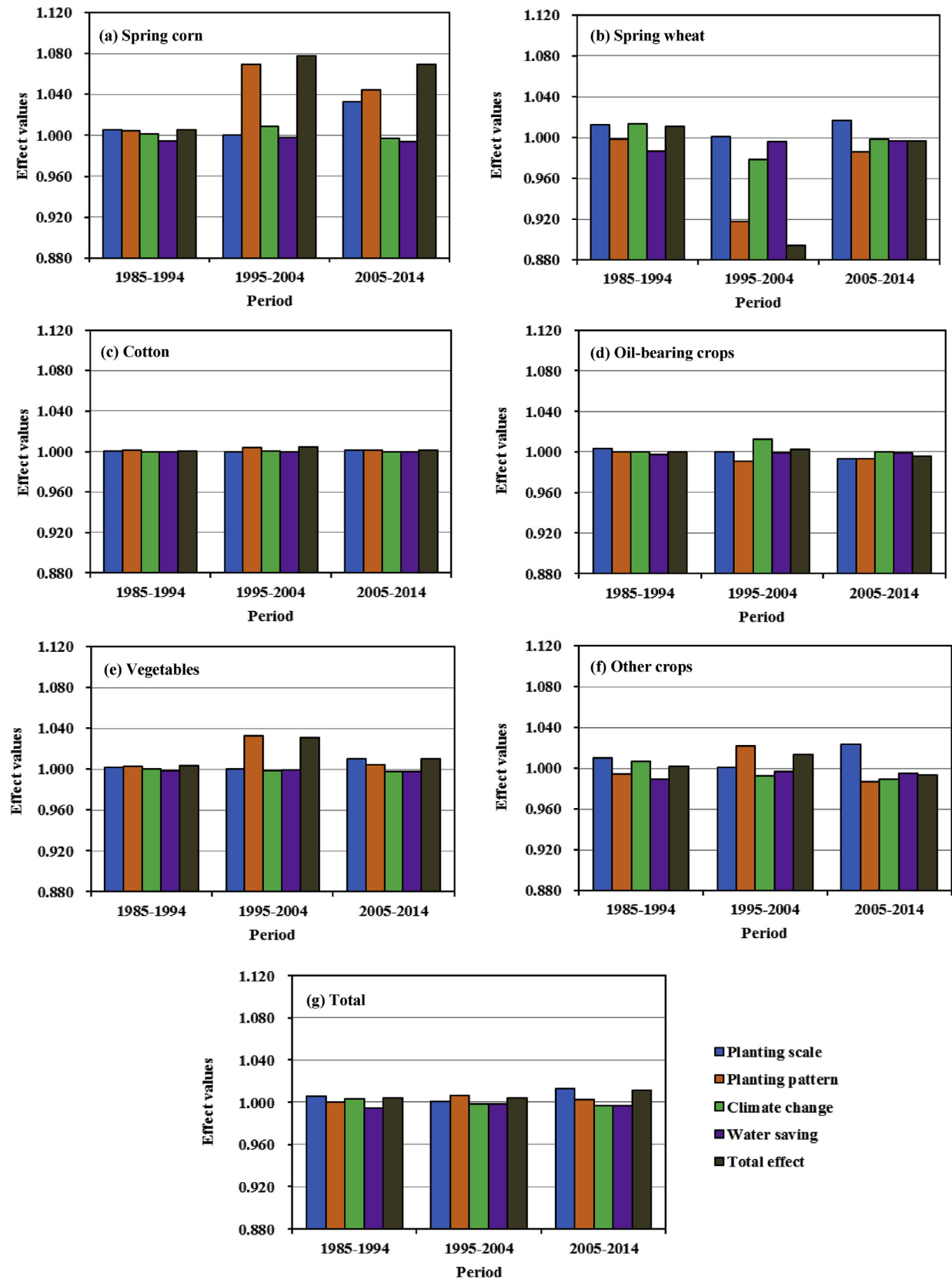


Fig. 8. Change in irrigation water demand for different crops using LMDI multiplicative decomposition.

1995–2004 and 2005–2014 is plain to see. The planting pattern raised irrigation water demand the most among the total effects in 1995–2004. The effects of the other decomposed factors were weak, but in the period 2005–2014, planting scale and planting patterns both exhibited strong impact. In addition, the irrigation water demand for spring wheat had declined since 1995 and the greatest reduction was in the period of 1995–2004, resulting in the total effect value of 0.894 (Fig. 8b). The main reason for this is that the proportion of the region that was planted with spring wheat significantly decreased after 1995. And the four factors all show a slightly increasing effect on irrigation water demand for cotton in the three periods with the relatively insignificant total effect (Fig. 8c). While for oil-bearing crops, the irrigation water demand first increased and then decreased, which is due to the major effect of the planting scale and planting pattern during the period 2005–2014. During this period of time, their total effect values were 0.993 and 0.994 (Fig. 8d), displaying a certain inhibitory effect of the planting scale and planting pattern on the irrigation water demand. Furthermore, the irrigation water demand for vegetables and other crops reached maximum values in the period 1995–2004, and the total effect values are 1.031 and 1.013 (Fig. 8e and f). This is largely resulting from the significant effect of planting pattern that raised irrigation water demand. However, the irrigation water demand for other crops showed a clear decreasing trend from 2005 to 2014. Note the total effect value was 0.993. Planting pattern, climate change and water saving technology were the factors that mainly influenced irrigation water demand during this period, all of which displayed a distinct decreasing trend.

Interestingly, the effect values of planting scale and planting pattern on the main crops in the study area were greater than 1, and the effect value of water saving technology was <1 in each period (Fig. 8g). This further suggests that, in order to reduce agricultural irrigation water consumption in this region, it is necessary to reduce the scale of cultivation and implement rational adjustment to the planting pattern in a large-scale. For example, when reducing the planting area of corn and vegetable, government decision makers should also actively encourage farmers to plant some coarse grain crops that require relatively low water demand. To form the diversity of planting patterns and models, it is also necessary to properly plan the cultivated scale and distribute bulk crops. Fig. 8g also shows that water saving projects and technologies in recent years have played a more important role in improving the efficient utilization of agricultural water resources. In the future, to further achieve higher efficiency of agricultural water use, the modern water-saving technologies can be combined with other agricultural approaches such as mulching or the efficiency of precipitation utilization is improved. Generally, climate change in each period first increased and then reduced irrigation water demand. These changes mainly resulted from more precipitation, higher air humidity and lower potential crop water demand in recent years (Zou et al., 2017). Climate change will disrupt water supply regime and may cause extreme hydrological events, which may cast impacts on the vulnerable Heihe River basin (Zhang et al., 2015d). Consequently, the oasis agriculture may gradually become unstable. Thus, the change of agricultural water consumption caused by climate change should be carefully managed.

#### 4.4. Uncertainty analysis

The decomposition results are comprehensive and it can provide a variety of results of the form when the LMDI decomposition method is used to analyze irrigation water demand. It is also possible to compare the effects of various driving factors on regional irrigation water demand, and to evaluate the results of planting scale effect, planting pattern effect, climate change effect

and water saving effect on irrigation water demand. Although LMDI provides a quantitative decomposition of the driving factors, there is still uncertainty in the results and a need for more in-depth analysis. First of all, the influencing factors directly or indirectly related to irrigation water demand can be taken into account when the LMDI decomposition method is adopted. Due to limited data, driving factors directly related to irrigation water demand were considered in this study. We did not consider other factors, such as changes in the planted crop varieties, cultivation and tillage practices, the use of plastic film mulch, groundwater extraction, or other difficult-to-quantify impact factors. These factors may need thorough investigation in the future.

The next concern is that driving factor values calculated in this study were not verified by real data because of the lack of experiment. The driving factor values are also needed to be compared with those produced from other decomposition models in future research to obtain more accurate results.

Finally, driving factors were analyzed over a historical period without including future uncertainties caused by climate change. Potential future changes of crop breeding and other possibilities have not been illustrated in this study and they can form the framework for future research endeavors.

Despite some uncertainties in this study, it is urgent and necessary to identify an accurate model to monitor changes in irrigation water demand. Based on this model, the contribution rate of each driving factor for the upper and middle reaches of Heihe River basin could be accurately estimated by considering the background of global climate change and intense human activity. Our results provide the valuable reference for improving management of agricultural irrigation water and scientific guidance on how to offset the increasingly severe conflict in agricultural and ecological water consumption.

## 5. Conclusions

This study constructed a SWAT model in the upper and middle reaches of Heihe River basin and incorporated the distributed hydrological response units to integrate hydrological simulation components to improve the method of estimating regional irrigation water demand. This enables us to quantify the temporal and spatial characteristics of irrigation water demand for each crop in the region from 1985 to 2014. Finally, two forms of LMDI factor decomposition (additive and multiplicative) were used to quantify the effects of four factors on demand for irrigation water, aiming to find an effective way to reduce irrigation water demand. The main conclusions are:

- (1) The SWAT model accurately simulates the hydrological components and provides precise estimates of regional crop irrigation water demand. Total irrigation water demand in the study region increased significantly from 1985 to 2014 with the average growth rate of  $0.453 \times 10^8 \text{ m}^3/\text{year}$  in the 30 year period. The irrigation water demand for spring corn, cotton, vegetables and other crops increased, and the irrigation water demand for spring wheat and oil-bearing crops decreased, indicating that the agricultural water supply in the region is unlikely to meet the demand.
- (2) The decomposition results of the total irrigation water demand that were quantified by the additive decomposition method from 1985 to 2014 suggest that planting scale, planting pattern and climate change increased irrigation water demand, while the water saving technology decreased irrigation water demand. The contribution of irrigation water demand values for planting scale, planting pattern, climate change and water saving technology were  $1.981 \times 10^8 \text{ m}^3$ ,

$0.933 \times 10^8 \text{ m}^3$ ,  $1.523 \times 10^8 \text{ m}^3$  and  $-1.188 \times 10^8 \text{ m}^3$ , respectively. Correspondingly, the average contribution rates of these driving factors were 60.96%, 28.72%, 46.86% and -36.53%, respectively.

- (3) The effects of planting scale, planting pattern, climate change and water saving on the irrigation water demand for each crop in three periods were different, but on the whole the scale and pattern of planting increased irrigation water demand, whereas the use of water saving technology reduced it. In order to reduce agricultural irrigation water consumption in the region, the planting pattern must be adjusted by reducing the area of crops that consume relatively large amounts of water, such as spring corn and vegetables, and simultaneously reducing the scale at which such crops are planted. In recent years, improvements in water saving projects and technologies have played a greater role in achieving the efficiency of agricultural water usage, which however still on its way. Climate change in each period clearly at first increased and then decreased the demand for irrigation water. This impact should be considered in the management of the supply of irrigation demand water.

## Acknowledgements

This study was supported by the Chinese National Natural Science Foundation Program (51621061, 91425302), the Special Fund for Agro-scientific Research in the Public Interest (201503125), and the Discipline Innovative Engineering Plan (111 Program, B14002).

## Appendix A. Supplementary data

Supplementary data related to this article can be found at <https://doi.org/10.1016/j.jclepro.2018.03.056>.

## References

- Abbaspour, K.C., Yang, J., Maximov, I., Siber, R., Bogner, K., Mieleitner, J., Zobrist, J., Srinivasan, R., 2007. Modelling hydrology and water quality in the pre-alpine/alpine Thur watershed using SWAT. *J. Hydrol.* 333 (2–4), 413–430.
- Ang, B.W., Zhang, F.Q., Choi, K.H., 1998. Factorizing changes in energy and environmental indicators through decomposition. *Energy* 23 (6), 489–495.
- Ang, B.W., 2015. LMDI decomposition approach: a guide for implementation. *Energy Pol.* 86, 233–238.
- Arnold, J.G., Srinivasan, R., Muttiah, R.S., Williams, J.R., 1998. Large area hydrologic modeling and assessment part I: model development. *J. Am. Water Resour. Assoc.* 34 (1), 73–89.
- Cheng, H., Hu, Y.A., Zhao, J.F., 2009. Meeting China's water shortage crisis: current practices and challenges. *Environ. Sci. Technol.* 43 (2), 240–244.
- Chong, C.H., Ma, L.W., Li, Z., Ni, W.D., Song, S.Z., 2015. Logarithmic mean division index (LMDI) decomposition of coal consumption in China based on the energy allocation diagram of coal flows. *Energy* 85, 366–378.
- Chung, S.O., Rodríguez-Díaz, J.A., Weatherhead, E.K., Knox, J.W., 2011. Climate change impacts on water for irrigating paddy rice in South Korea. *Irrig. Drain.* 60 (2), 263–273.
- Díaz, J.A.R., Weatherhead, E.K., Knox, J.W., Camach, E., 2007. Climate change impacts on irrigation water requirements in the Guadalquivir river basin in Spain. *Reg. Environ. Change* 7 (3), 149–159.
- Doorenbos, J., Pruitt, W.O., 1977. Guidelines for Predicting Crop Water Requirements. Food and Agriculture Organization of the United Nations. Water Resources and Development Service, Rome, p. 144.
- Du, T.S., Kang, S.Z., Zhang, J.H., Davies, W.J., 2015. Deficit irrigation and sustainable water-resource strategies in agriculture for China's food security. *J. Exp. Bot.* 66 (8), 2253–2269.
- Duan, A.W., Sun, J.S., Liu, Y., Xiao, J.F., Liu, Q.C., Qi, X.B., 2004. Irrigation Quota of Major Crops for Northern China. China Agricultural Science & Technology Press, Beijing, p. 197.
- Gassman, P.W., Reyes, M.R., Green, C.H., Arnold, J.G., 2007. The soil and water assessment tool: historical development, applications, and future research directions. *Trans. ASABE (Am. Soc. Agric. Biol. Eng.)* 50 (4), 1211–1250.
- Guo, Y., Shen, Y.J., 2016. Agricultural water supply/demand changes under projected future climate change in the arid region of northwestern China. *J. Hydrol.* 540, 257–273.
- Hao, Z.C., Zhang, Y.G., Yang, C.G., Li, J.W., Dawa, T., 2013. Effects of topography and snowmelt on hydrologic simulation in the Yellow River's source region. *Adv. Water Sci.* 24 (3), 311–318 in Chinese).
- Hu, W., Yan, C.R., Li, Y.C., Liu, Q., 2014. Impacts of climate change on winter wheat growing period and irrigation water requirements in the north China plain. *Acta Ecol. Sin.* 34 (9), 2367–2377 in Chinese).
- Kang, S.Z., Hao, X.M., Du, T.S., Tong, L., Su, X.L., Lu, H.N., Li, X.L., Huo, Z.L., Li, S.E., Ding, R.S., 2017. Improving agricultural water productivity to ensure food security in China under changing environment: from research to practice. *Agric. Water Manage.* 179, 5–17.
- Kannan, N., Santhi, C., Arnold, J.G., 2008. Development of an automated procedure for estimation of the spatial variation of runoff in large river basins. *J. Hydrol.* 359 (1–2), 1–15.
- Kendall, M., Stuart, A., 1964. The Advanced Theory of Statistics. Charles Griffin, London.
- Lei, H.J., Xia, X.F., Li, C.J., Xi, B.D., 2012. Decomposition analysis of wastewater pollutant discharges in industrial sectors of China (2001–2009) using the LMDI I Method. *Int. J. Environ. Res. Public Health* 9 (6), 2226–2240.
- Li, Z.L., Shao, Q.X., Xu, Z.X., Cai, X.T., 2010. Analysis of parameter uncertainty in semi-distributed hydrological models using bootstrap method: a case study of SWAT model applied to Yingluoxia watershed in northwest China. *J. Hydrol.* 385 (1–4), 76–83.
- Li, J., Zhu, T., Mao, X.M., Adedoye, A.J., 2016. Modeling crop water consumption and water productivity in the middle reaches of Heihe River Basin. *Comput. Electron. Agric.* 123 (C), 242–255.
- Liu, Y.C., Jiang, H.A., Li, C.D., Huang, H., Pan, Z.H., Cai, C.L., 2013. Analysis of irrigation water requirement and irrigation requirement index for cotton of Hebei province. *Trans. Chin. Soc. Agric. Eng.* 29 (19), 98–104 in Chinese).
- Lu, Z.X., Zou, S.B., Xiao, H.L., Zheng, C.M., Yin, Z.L., Wang, W.H., 2015. Comprehensive hydrologic calibration of Swat and water balance analysis in mountainous watersheds in northwest China. *Phys. Chem. Earth* 76–85, s79–82.
- Ma, L., Yang, Y.M., Yang, Y.H., Xiao, D.P., Bi, S.J., 2011. The distribution and driving factors of irrigation water requirements in the North China Plain. *J. Remote Sens.* 15 (2), 324–339.
- Ma, L.H., Kang, S.Z., Su, X.L., Tong, L., 2012. Simulation and uncertainty analysis of net irrigation requirement in agricultural area. *Trans. Chin. Soc. Agric. Eng.* 28 (8), 11–18 in Chinese).
- Mann, H.B., 1945. Nonparametric tests against trend. *Econometrica* 13 (3), 245–259.
- Mohan, S., Simhadri, B., Arumugam, N., 1996. Comparative study of effective rainfall estimation methods for lowland rice. *Water Resour. Manage.* 10 (1), 35–44.
- Moriasi, D.N., Arnold, J.G., van Liew, M.W., Bingner, R.L., Harmel, R.D., Veith, T.L., 2007. Model evaluation guidelines for systematic quantification of accuracy in watershed simulations. *Trans. ASABE (Am. Soc. Agric. Biol. Eng.)* 50, 885–900.
- Neitsch, S.L., Arnold, J.G., Kiniry, J.R., Williams, J.R., King, K.W., 2002. Soil and Water Assessment Tool. Theoretical Documentation. Texas Water Resources Institute, College Station, Tex. TWRIR-191, Version 2000.
- Neitsch, S.L., Arnold, J.G., Kiniry, J.R., Williams, J.R., 2005. Soil and Water Assessment Tool. Theoretical Documentation. Grassland, Soil and Water Research Laboratory, Agricultural Research Service and Blackland Research Center: Texas Agricultural Experiment Station, Temple, Tex, Version 2005.
- Pettitt, A.N., 1979. A non-parametric approach to the change-point problem. *J. R. Stat. Soc. C: Appl. Stat.* 28 (2), 126–135.
- Shen, Y.J., Li, S., Chen, Y.N., Qi, Y.Q., Zhang, S.W., 2013. Estimation of regional irrigation water requirement and water supply risk in the arid region of northwestern China 1989–2010. *Agric. Water Manage.* 128 (10), 55–64.
- Tomohisa, Y., Mehmet, A., Tomokazu, H., 2007. Impact of climate change on irrigation demand and crop growth in a mediterranean environment of Turkey. *Sensors* 7 (10), 2297–2315.
- Tursun, H., Li, Z.Y., Liu, R., Li, Y., Wang, X.H., 2015. Contribution weight of engineer technology on pollutant emission reduction based on IPAT and LMDI methods. *Clean Techn. Environ. Policy* 17 (1), 225–235.
- van Griensven, A., Meixner, T., Grunwald, S., Bishop, T., Diluzio, M., Srinivasan, R., 2006. A global sensitivity analysis tool for the parameters of multi-variable catchment models. *J. Hydrol.* 324 (1–4), 10–23.
- Vorosmarty, C.J., Green, P., Salisbury, J., Lammers, R.B., 2000. Global water resources: vulnerability from climate change and population growth. *Science* 289 (5477), 284–288.
- Wu, Y.P., Chen, J., 2013. Estimating irrigation water demand using an improved method and optimizing reservoir operation for water supply and hydropower generation: a case study of the xinfengjiang reservoir in southern China. *Agric. Water Manage.* 116 (116), 110–121.
- Wu, X.J., Zhou, J., Wang, H.J., Li, Y., Zhong, B., 2015. Evaluation of irrigation water use efficiency using remote sensing in the middle reach of the Heihe river, in the semi-arid Northwestern China. *Hydrol. Process.* 29, 2243–2257.
- Xie, J., Su, X.L., 2017. Decomposition of influencing factors on irrigation water requirement based on LMDI method. *Trans. Chin. Soc. Agric. Eng.* 33 (7), 123–131 in Chinese).
- Xu, Y.J., Huang, K., Yu, Y.J., Wang, X.M., 2015. Change in water footprint of crop production in Beijing from 1978 to 2012: a logarithmic mean Divisia index decomposition analysis. *J. Clean. Prod.* 87, 180–187.
- Zhang, X.S., Srinivasan, R., Van Liew, M., 2010. On the use of multi-algorithm, genetically adaptive multi-objective method for multi-site calibration of the SWAT model. *Hydrol. Process.* 24 (8), 955–969.
- Zhang, L.B., Xu, Y.J., Jin, J.L., Wu, C.G., 2014. Analysis of influence factors of regional industry water use in Anhui province. *J. Hydraul. Eng.* 45 (7), 837–843 in Chinese).

- Zhang, A.J., Zheng, C.M., Wang, S., Yao, Y.Y., 2015a. Analysis of streamflow variations in the heihe river basin, northwest China: trends, abrupt changes, driving factors and ecological influences. *J. Hydrol.: Reg. Stud.* 3 (C), 106–124.
- Zhang, L., Nan, Z.T., Yu, W.J., Ge, Y.C., 2015b. Modeling land-use and land-cover change and hydrological responses under consistent climate change scenarios in the heihe river basin, China. *Water Resour. Manage.* 29 (13), 4701–4717.
- Zhang, Y.F., Yang, D.G., Tang, H., Liu, Y.X., 2015c. Analyses of changing process and influencing factors of water resources utilization in megalopolis of arid area. *Water Resour.* 42 (5), 712–720.
- Zhang, Y.Y., Fu, G.B., Sun, B.Y., Zhang, S.F., Men, B.H., 2015d. Simulation and classification of the impacts of projected climate change on flow regimes in the arid Hexi Corridor of Northwest China. *J. Geophys. Res. Atmos.* 120, 7429–7453.
- Zhang, A.J., Liu, W.B., Yin, Z.L., Fu, G.B., Zheng, C.M., 2016a. How will climate change affect the water availability in the Heihe river basin, Northwest China? *J. Hydromet.* 17 (5), 1517–1542.
- Zhang, L., Nan, Z.T., Yu, W.J., Ge, Y.C., 2016b. Hydrological responses to land-use change scenarios under constant and changed climatic conditions. *Environ. Manage.* 57 (2), 412–431.
- Zhang, W., Li, K., Zhou, D.Q., Zhang, W.R., Gao, H., 2016c. Decomposition of intensity of energy-related CO<sub>2</sub> emission in Chinese provinces using the LMDI method. *Energy Pol.* 92, 369–381.
- Zhao, C.F., Chen, B., 2014. Driving force analysis of the agricultural water footprint in China based on the LMDI method. *Environ. Sci. Technol.* 48 (21), 12723–12731.
- Zou, M.Z., Niu, J., Kang, S.Z., Li, X.L., Lu, H.N., 2017. The contribution of human agricultural activities to increasing evapotranspiration is significantly greater than climate change effect over Heihe agricultural region. *Sci. Rep.* 7, 8805. <https://doi.org/10.1038/s41598-017-08952-5>.

## List of symbols

### Symbols, Implication, Units

- $A_{ij}$ : The planted area for crop  $i$  in year  $j$ ,  $10^4$  ha
- $A_j$ : The planted area in year  $j$ ,  $10^4$  ha
- $c_p$ : The specific heat at constant pressure,  $\text{MJ kg}^{-1} \text{ } ^\circ\text{C}^{-1}$
- $D_{tot}$ : The ratio of irrigation water demand for year  $j$  to the base year
- $D_A$ : The planting scale factor
- $D_a$ : The planting pattern factor
- $D_C$ : The water saving technology factor
- $D_I$ : The climate change factor
- $e_z$ : The water vapor pressure of air at height  $z$ , kPa

- $e_z^0$ : The saturation vapor pressure of air at height  $z$ , kPa
- $E_b$ : The elevation of the mid-point elevation of the altitude zone  $b$ , km
- $E_{gage}$ : The elevation of the weather station, km
- $ET$ : Crop water demand for each growing season, mm
- $ET_0$ : Potential crop water demand during the growing season, mm
- $G$ : Heat flux density to the ground,  $\text{MJ m}^{-2} \text{ d}^{-1}$
- $H_{net}$ : Net radiation,  $\text{MJ m}^{-2} \text{ d}^{-1}$
- $I$ : Net irrigation water demand, mm
- $I_{ij}$ : The net irrigation water demand per unit area of crop  $i$  in year  $j$ , mm
- $K_c$ : Crop coefficient
- $LATQ$ : Subsurface lateral flow (flowing out of the root zone and entering the river), mm
- $P$ : The precipitation recorded at the weather station, mm
- $P_b$ : The precipitation in altitude zone  $b$ , mm
- $P_e$ : The effective precipitation, mm
- $P_{laps}$ : The lapse rate of precipitation,  $\text{mm km}^{-1}$
- $PREP$ : The amount of precipitation reaching the soil surface, mm
- $r_a$ : The diffusion resistance of the air layer (aerodynamic resistance),  $\text{S m}^{-1}$
- $r_c$ : The crop canopy resistance,  $\text{S m}^{-1}$
- $S$ : The planted area of the crop,  $10^4$  ha
- $SEEP$ : Seepage from the bottom of the soil profile, mm
- $SURQ$ : Surface streamflow, mm
- $T_{b,max}$ : The maximum temperature of altitude zone  $b$ ,  $^\circ\text{C}$
- $T_{b,min}$ : The minimum temperature of altitude zone  $b$ ,  $^\circ\text{C}$
- $T_{laps}$ : The lapse rate of temperature,  $^\circ\text{C km}^{-1}$
- $T_{max}$ : The maximum temperature of the weather station,  $^\circ\text{C}$
- $T_{min}$ : The minimum temperature of the weather station,  $^\circ\text{C}$
- $W$ : Gross irrigation water demand,  $10^8 \text{ m}^3$
- $W_{ij}$ : Gross irrigation water demand for crop  $i$  in year  $j$ ,  $10^8 \text{ m}^3$
- $W^0$ : The irrigation water demand for the base year,  $10^8 \text{ m}^3$
- $W^j$ : The irrigation water demand for year  $j$ ,  $10^8 \text{ m}^3$
- $\Delta W_{tot}$ : The change in irrigation water demand,  $10^8 \text{ m}^3$
- $\Delta W_A$ : The effect of changes in planting scale,  $10^8 \text{ m}^3$
- $\Delta W_a$ : The effect of changes in planting patterns,  $10^8 \text{ m}^3$
- $\Delta W_C$ : The effect of changes in water saving technology,  $10^8 \text{ m}^3$
- $\Delta W_I$ : The effect of climate change,  $10^8 \text{ m}^3$
- $w_{ij}$ : Net irrigation water demand for crop  $i$  in year  $j$ ,  $10^8 \text{ m}^3$
- $\Delta$ : The slope of the saturation vapor pressure curve at air temperature,  $\text{kPa } ^\circ\text{C}^{-1}$
- $\rho_{air}$ : Air density,  $\text{kg m}^{-3}$
- $\gamma$ : The psychrometric constant,  $\text{kg m}^{-3}$
- $\eta$ : The irrigation water use efficiency
- $\eta_j$ : The irrigation water use efficiency for year  $j$
- $\alpha_{ij}$ : The ratio of the planted area of crop  $i$  to the total area in year  $j$